Wilfried Elmenreich, J. Tenreiro Machado and Imre J. Rudas (Eds)

Intelligent Systems

at the Service of Mankind

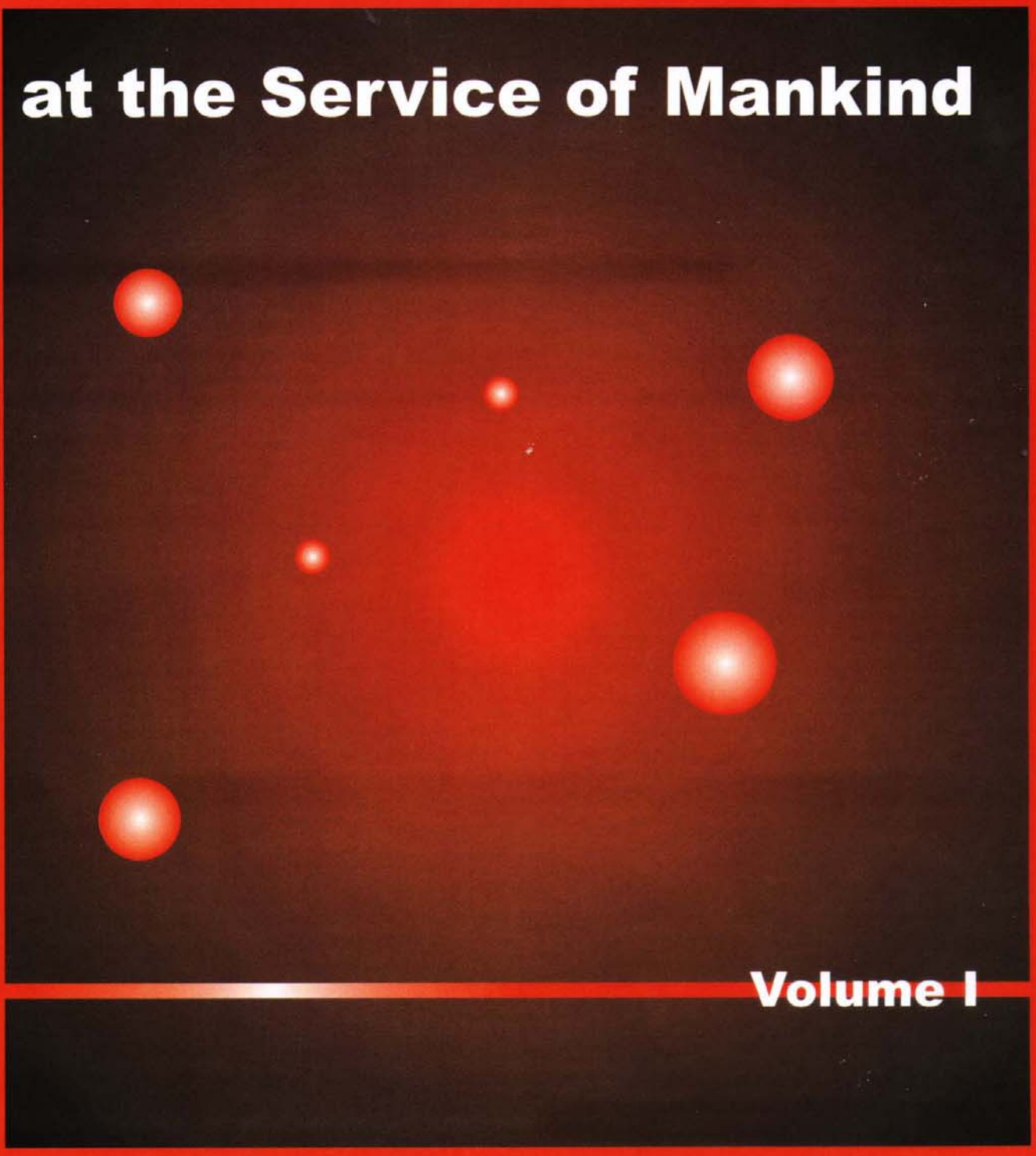

Volume I

Gait Analysis of Natural and Artificial Walking Systems

Manuel F. Silva[1], J. A. Tenreiro Machado[1], and António M. Lopes[2]

[1]Department of Electrical Engineering,
Institute of Engineering of Porto, Porto, Portugal
{mfsilva,jtm}@dee.isep.ipp.pt

[2]Department of Mechanical Engineering,
Faculty of Engineering of Porto, Porto, Portugal
aml@fe.up.pt

Abstract — *This paper studies periodic gaits of multi-legged locomotion systems based on dynamic models. The purpose is to determine the system performance during walking and the best set of locomotion variables. For that objective the prescribed motion of the robot is completely characterized in terms of several locomotion variables such as gait, duty factor, body height, step length, stroke pitch, foot clearance, legs link lengths, foot-hip offset, body and legs mass and cycle time. In this perspective, we formulate three performance measures of the walking robot namely, the mean absolute energy, the mean power dispersion and the mean power lost in the joint actuators per walking distance. A set of model-based experiments reveals the influence of the locomotion variables in the proposed indices.*

1 Introduction

Walking machines allow locomotion in terrain inaccessible to other type of vehicles, since they do not need a continuous support surface [1]. On the other hand, the requirements for leg coordination and control impose difficulties beyond those encountered in wheeled robots [2]. Gait selection is a research area requiring an appreciable modeling effort for the improvement of mobility with legs in unstructured environments [3,4]. Previous studies mainly focused in the structure and selection of locomotion modes [5 – 9]. Nevertheless, there are different optimization criteria such as energy efficiency [10], stability [2], velocity [11,12], comfort, mobility [13] and environmental impact. With these facts in mind, a simulation model for multi-leg locomotion systems was developed, for several periodic gaits. This study intends to generalize previous work [14 – 16] through the formulation of several dynamic indices measuring the average energy during different walking trajectories, the mean power dispersion and the power lost in the joint actuators along the space-time walking cycle.

The foot and body trajectories are analyzed in what concerns its variation with the gait, duty factor, step length, maximum foot clearance, body height, legs link lengths and foot trajectory offset. Several simulation experiments reveal the system configuration and the type of the movements that lead to a better mechanical implementation, for a given locomotion mode, from the viewpoint of the proposed indices.

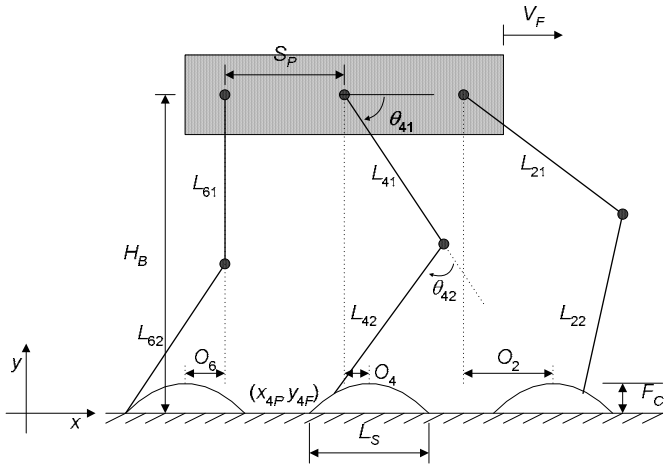

Figure 1: Coordinate system and variables that characterize the motion trajectories of the multi-legged robot

Bearing these facts in mind, the paper is organized as follows. Section two introduces the model for a multi-legged robot and the motion planning algorithms. Section three formulates the optimizing indices and section four develops a set of experiments that reveal the influence of the system parameters in the periodic gaits, respectively. Finally, section five presents the main conclusions and directions towards future developments.

2 A Model for Multi-legged Locomotion

We consider a longitudinal walking system with n legs ($n \geq 2$ and n even), with the legs equally distributed along both sides of the robot body, having each one two rotational joints (Figure 1).

Motion is described by means of a world coordinate system. The kinematic model comprises: the cycle time T, the duty factor β, the transference time $t_T = (1-\beta)T$, the support time $t_S = \beta T$, the step length L_S, the stroke pitch S_P, the body height H_B, the maximum foot clearance F_C, the i^{th} leg lengths L_{i1} and L_{i2} and the foot trajectory offset O_i (i=1,…,n). Moreover, we consider a periodic trajectory for each foot, with body velocity $V_F = L_S / T$.

The algorithm for the forward motion planning accepts the body and i^{th} feet desired cartesian trajectories $\mathbf{p_{Fd}}(t) = [x_{iFd}(t), y_{iFd}(t)]^{\text{T}}$ as inputs and, by means of an inverse kinematics algorithm, generates the related joint trajectories $\boldsymbol{\theta}_\mathbf{d}(t) = [\theta_{i1d}(t), \theta_{i2d}(t)]^{\text{T}}$, selecting the solution corresponding to a forward knee.

The body of the robot, and by consequence the legs hips, is assumed to have a desired horizontal movement with a constant forward speed V_F. Therefore, for leg i the cartesian coordinates of the hip of the legs are given by:

$$\mathbf{p_{Hd}}(t) = \begin{bmatrix} x_{iHd}(t) \\ y_{iHd}(t) \end{bmatrix} = \begin{bmatrix} V_F t \\ H_B \end{bmatrix} \tag{1}$$

Given a particular gait and duty factor β, it is possible to calculate for leg i the corresponding phase ϕ_i and the time instant where each leg leaves and returns to contact with the ground [2]. From these results, and knowing T, β and t_S, the cartesian trajectories of the tip of the foots must be completed during t_T.

For each cycle the desired trajectory of the tip of the swing leg is computed through a cycloid function given by (considering, for example, that the transfer phase starts at

t = 0 s for leg 1), with $f = 1/T$:

— during the transfer phase:

$$x_{1Fd}(t) = V_F\left[t - \frac{1}{2\pi f}\sin\left(2\pi ft\right)\right] \tag{2a}$$

$$y_{1Fd}(t) = \frac{F_C}{2}\left[1 - \cos\left(2\pi ft\right)\right] \tag{2b}$$

— during the stance phase:

$$x_{1Fd}(t) = V_F T \tag{3a}$$

$$y_{1Fd}(t) = 0 \tag{3b}$$

From the coordinates of the hip and feet of the robot it is possible to obtain the leg joint positions and velocities using the inverse kinematics $\boldsymbol{\psi}^{-1}$ and the Jacobian $\mathbf{J} = \partial\boldsymbol{\psi}/\partial\boldsymbol{\theta}$ yielding:

$$\mathbf{p_d}(t) = \begin{bmatrix} x_{id}(t) \\ y_{id}(t) \end{bmatrix} = \mathbf{p_{Hd}}(t) - \mathbf{p_{Fd}}(t) \tag{4a}$$

$$\mathbf{p_d}(t) = \boldsymbol{\psi}\left[\boldsymbol{\theta}_\mathbf{d}(t)\right] \Rightarrow \boldsymbol{\theta}_\mathbf{d}(t) = \boldsymbol{\psi}^{-1}\left[\mathbf{p_d}(t)\right] \tag{4b}$$

$$\dot{\boldsymbol{\theta}}_\mathbf{d}(t) = \mathbf{J}^{-1}\left[\dot{\mathbf{p}}_\mathbf{d}(t)\right] \tag{4c}$$

Based on this data, the trajectory generator is responsible for producing a motion that synchronises and co-ordinates the legs. In order to avoid the impact and friction effects, at the planning phase we estimate null velocities of the feet in the instants of landing and taking off, assuring also the velocity continuity.

These joint trajectories can also be accomplished either with a step or a polynomial *versus* time acceleration profile. After planning the joint trajectories we calculate the inverse dynamics in order to 'map' the kinematics into power consumption. The robot inverse dynamic model is of the form:

$$\boldsymbol{\tau} = \mathbf{H}(\boldsymbol{\theta})\ddot{\boldsymbol{\theta}} + \mathbf{c}\left(\boldsymbol{\theta}, \dot{\boldsymbol{\theta}}\right) + \mathbf{g}(\boldsymbol{\theta}) \tag{5}$$

where $\boldsymbol{\tau} = [f_{ix}, f_{iy}, \tau_{i1}, \tau_{i2}]^\mathrm{T}$ (i=1,…,n) is the vector of forces/torques, $\boldsymbol{\theta} = [x_{iH}, y_{iH}, \theta_{i1}, \theta_{i2}]^\mathrm{T}$ is the vector of position coordinates, $\mathbf{H}(\boldsymbol{\theta})$ is the inertia matrix and $\mathbf{c}\left(\boldsymbol{\theta}, \dot{\boldsymbol{\theta}}\right)$ and $\mathbf{g}(\boldsymbol{\theta})$ are the vectors of centrifugal/Coriolis and gravitational forces/torques, respectively.

3 Measures for Performance Evaluation

In mathematical terms, we provide three global measures of the overall performance of the mechanism in an average sense.

3.1 Mean Absolute Energy

A first measure in this analysis is the mean absolute energy per travelled distance. It is computed assuming that energy regeneration is not available by actuators doing negative work, that is, by taking the absolute value of the energy. At a given joint j (each leg has m = 2 joints) and leg i, the mechanical power is the product of the motor torque and angular velocity. The global index is obtained by averaging the mechanical

absolute energy delivered over the step length L_S:

$$E_{av} = \frac{1}{L_S} \sum_{i=1}^{n} \sum_{j=1}^{m} \int_0^T \left| \boldsymbol{\tau}_{ij}(t) \cdot \dot{\boldsymbol{\theta}}_{ij}(t) \right| dt \tag{6}$$

The average of the absolute energy consumption, per travelled distance, E_{av}, should be minimised.

3.2 Mean Power Dispersion

Although minimising energy appears to be an important consideration, it may occur instantaneous, very high, power demands. In such cases, the average value can be small while the peaks are physically unrealisable. An alternative index is the standard deviation per meter that evaluates the dispersion around the mean absolute energy over a complete cycle T and step length L_S:

$$P_i(t) = \sum_{i=1}^{n} \sum_{j=1}^{m} \left| \boldsymbol{\tau}_{ij}(t) \cdot \dot{\boldsymbol{\theta}}_{ij}(t) \right| \tag{7a}$$

$$D_{av} = \frac{1}{L_S} \cdot \sqrt{\frac{1}{T} \int_0^T \left[P_i(t) - E_{av} \right]^2 dt} \tag{7b}$$

where P_i is the total instantaneous absolute mechanical power. In this line of thought, the most suitable trajectory is the one that minimizes D_{av}.

3.2 Mean Power Lost

Another alternative optimisation strategy addresses the power lost in the joint actuators per step length L_S. From this point of view, the index mean power lost per meter can be defined as:

$$T_L = \frac{1}{L_S} \sqrt{\sum_{i=1}^{n} \sum_{j=1}^{m} \int_0^T \left[\boldsymbol{\tau}_{ij}(t) \right]^2 dt} \tag{8}$$

The most suitable trajectory is the one that minimizes T_L.

4 Simulation Results

To illustrate the use of the preceding concepts, in this section we develop a set of simulation experiments to estimate the influence of several parameters during periodic gaits and to compare the performance measures. Consequently, the multi-legged locomotion was simulated, in order to examine the role of the walking gait *versus* β, L_S, H_B and F_C, with $n = 6$, $V_F = 1$ ms^{-1}, $S_P = 1$ m, $L_{i1} = L_{i2} = 0.5$ m, $O_i = 0$ m, $M_b = 87.4$ kg, $M_{i1} = M_{i2} = 1.05$ kg and $M_{if} = 0$ kg.

Due to the high number of parameters and values, in the sequel we capture the optimal values by cross-relating several distinct combinations for the Wave Gait (*WG*):

— Step Length *vs.* Body Height – Figures 2 – 4 show E_{av}, D_{av} and T_L *versus* (L_S, H_B). We verify that all indices decrease slightly with H_B and sharply with L_S.

— Step Length *vs.* Duty Factor – Figures 5 – 7 depict the three indices *versus* (L_S, β). We conclude that E_{av}, D_{av} and T_L increase monotonically with β and decrease with L_S.

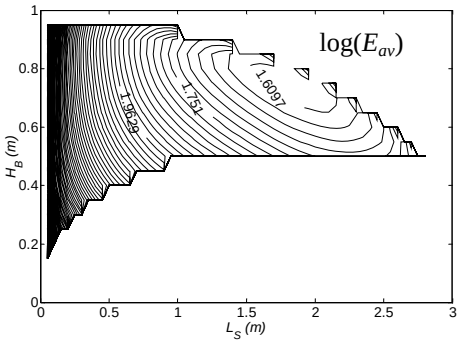

Figure 2: Plot of log(E_{av}) *vs.* (L_S, H_B) for β = 50%, F_C = 0.01 m, V_F = 1 ms^{-1}, *WG*

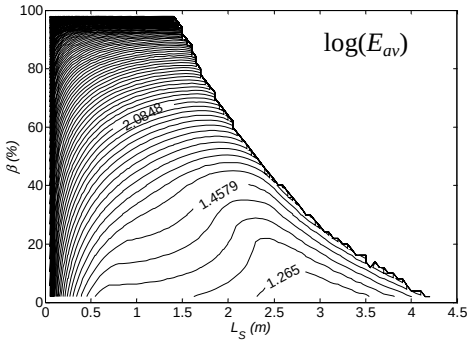

Figure 5: Plot of log(E_{av}) *vs.* (L_S, β) for F_C = 0.01 m, H_B = 0.7 m, V_F = 1 ms^{-1}, *WG*

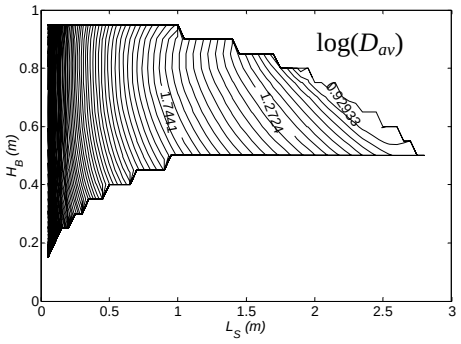

Figure 3: Plot of log(D_{av}) *vs.* (L_S, H_B) for β = 50%, F_C = 0.01 m, V_F = 1 ms^{-1}, *WG*

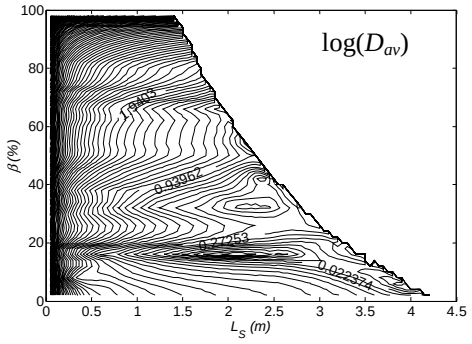

Figure 6: Plot of log(D_{av}) *vs.* (L_S, β) for F_C = 0.01 m, H_B = 0.7 m, V_F = 1 ms^{-1}, *WG*

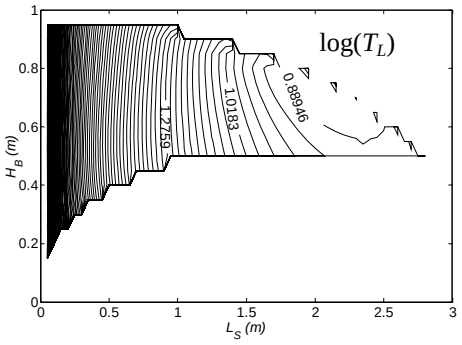

Figure 4: Plot of log(T_L) *vs.* (L_S, H_B) for β = 50%, F_C = 0.01 m, V_F = 1 ms^{-1}, *WG*

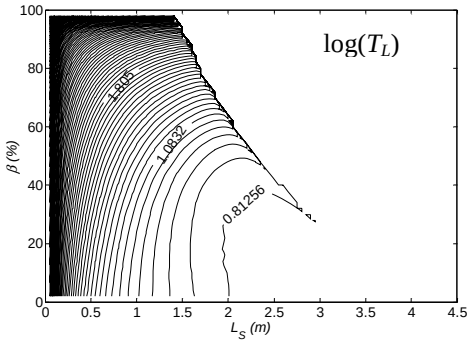

Figure 7: Plot of log(T_L) *vs.* (L_S, β) for F_C = 0.01 m, H_B = 0.7 m, V_F = 1 ms^{-1}, *WG*

— Duty Factor *vs.* Body Height – Figure 8 depicts $E_{av}(\beta, H_B)$. We conclude that E_{av} increases monotonically with β and decreases slightly with H_B. Although not presented $D_{av}(\beta, H_B)$ and $T_L(\beta, H_B)$ show the same type of variation with β and H_B.

— Duty Factor *vs.* Foot Clearance – Figure 9 depicts $E_{av}(\beta, F_C)$ revealing that it increases with β and F_C. The charts of $D_{av}(\beta, F_C)$ and $T_L(\beta, F_C)$ show the same type of variation with β and F_C.

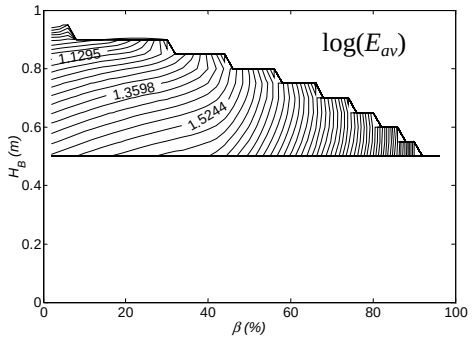

Figure 8: Plot of log(E_{av}) *vs.* (β, H_B) for L_S = 1.8 m, F_C = 0.01 m, V_F = 1 ms^{-1}, *WG*

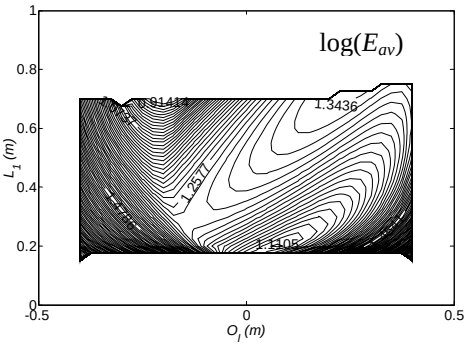

Figure 10: Plot of log(E_{av}) *vs.* (L_{i1}, O_i) for β = 2%, L_S = 1.8 m, F_C = 0.01 m, H_B = 0.7 m, V_F = 1 ms^{-1}, *WG*

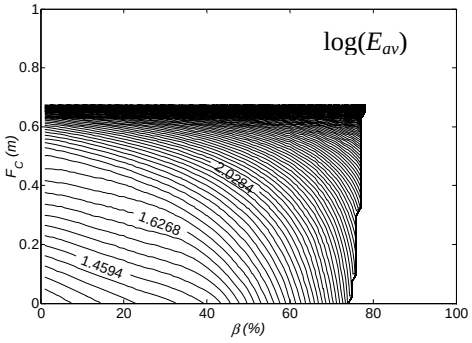

Figure 9: Plot of log(E_{av}) *vs.* (β, F_C) for L_S = 1.8 m, H_B = 0.7 m, V_F = 1 ms^{-1}, *WG*

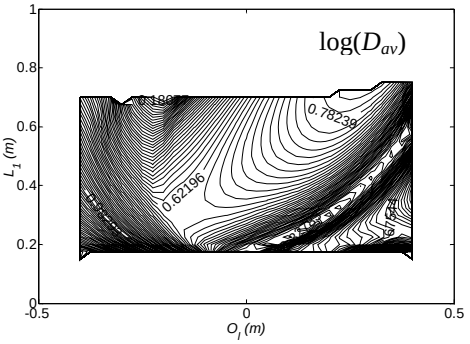

Figure 11: Plot of log(D_{av}) *vs.* (L_{i1}, O_i) for β = 2%, L_S = 1.8 m, F_C = 0.01 m, H_B = 0.7 m, V_F = 1 ms^{-1}, *WG*

— Foot Trajectory Offset *vs.* Leg Length – In the previous experiments we considered constant link lengths and masses, namely $L_{i1} = L_{i2} = 0.5$ m and $M_{i1} = M_{i2} = 1$ kg, for $O_i = 0$ m. Now we study the influence of these factors upon E_{av}, D_{av} and T_L. Therefore, we establish a total constant leg length and mass of $L_t = L_{i1} + L_{i2} = 1$ m and $M_{Lt} = M_{i1} + M_{i2} = 2$ kg while varying the relation between the two links, yielding (i = 1, …, 6; j = 1, 2) $M_{ij} = (L_{ij} / L_t).M_{Lt}$.
Figure 10 shows $E_{av}(O_i, L_{i1})$ for legs link lengths $0.0 < L_{i1} < 1.0$ and for hip–foot offset $-0.5 < O_i < 0.5$.
We verify that E_{av} varies slightly with L_{i1} and O_i. Log(D_{av}) – Figure 11 – and log(T_L) present a similar variation. Furthermore, it results that the locomotion is more efficient with $L_{i1} \approx 0.7$ m (L_{i1}+L_{i2} = 1 m) and $O_i \approx -0.2$ m.

In conclusion, comparing all the previous experiments, we can establish a compromise for optimising the Wave Gait, namely, that the best situation occurs for $\beta \approx 2\%$, $0.9 \le H_B \le 0.95$ m, $2.5 \le L_S \le 3.0$ m and $F_C \approx 0$ m, considering $L_{i1} = L_{i2} = 0.5$ m, $O_i = 0$ m and $V_F = 1$ ms^{-1} (it should be noted that this value of β corresponds to the robot working on a running condition rather than just walking).

Once established these optimal values we can study the effect of other parameters, namely:

— Body Forward Velocity – Figures 12 – 14 present the evolution of $\min[E_{av}(V_F)]$, $\min[D_{av}(V_F)]$ and $\min[T_L(V_F)]$, respectively. Figure 14 reveals that for low velocities we have $E_{av} \propto V_F^{-0.01}$ while for high velocities $E_{av} \propto V_F^{2.16}$. For medium velocities, this chart presents a transition area in the range $0.5 < V_F < 3.0$ ms^{-1}.
Concerning D_{av} we have a similar variation (Figure 15). For low velocities we have $D_{av} \propto V_F^{-0.04}$ while for high velocities $D_{av} \propto V_F^{3.32}$. For medium velocities, this chart presents a transition area in the range $0.2 < V_F < 3.0$ ms^{-1} with a minimum at $V_F \approx 1.0$ ms^{-1}.
The chart for T_L (Figure 16) presents a slightly different variation, being $T_L \propto V_F^{-0.51}$ for low velocities and $T_L \propto V_F^{1.65}$ for high velocities. For this index, the transitions occur in the range $0.9 < V_F < 3.0$ ms^{-1} and, in this case, we have $T_L \propto V_F^{-0.01}$.

— Body Height and Step Length *vs.* Body Forward Velocity – Figure 15 presents the evolution of $L_S(V_F)$ and $H_B(V_F)$ for the minimum values of E_{av}. We conclude that for $V_F \leq 3$ ms^{-1} L_S / H_B increases / decreases with V_F from $L_S = 1.0$ m / $H_B = 0.95$ m up to $L_S = 4.5$ m / $H_B = 0.6$ m. Moreover, $L_S(V_F)$ and $H_B(V_F)$ present the same variation for the minimum values of D_{av} and T_L.

— Number of Legs – In this case we consider two alternatives. A first option is to establish that each leg mass is constant and, therefore, the total robot mass (M_{Rt}) varies with the number of legs (n):

$$M_{Rt} = M_b + \sum_{i=1}^{n} \left(M_{i1} + M_{i2} \right), \; M_{i1} = M_{i2} = 1kg \tag{9}$$

where M_b is the mass of the body. Figure 16 shows that E_{av} increases proportionally with n. We get similar conclusions for D_{av} and T_L (Figures 17 and 18).
A second alternative is to have a robot with the total mass (M_{Rt}) constant:

$$M_{Rt} = M_b + \sum_{i=1}^{n} \left(M_{i1} + M_{i2} \right), \; M_{Rt} = 100\,kg \tag{10}$$

The legs mass varies with n, according to the expression [17 – 19]:

$$\frac{\left(M_{i1} + M_{i2} \right)}{M_{Rt}} = 0.35 e^{-0.47n}, \; M_{i1} = M_{i2}, \; \forall i \tag{11}$$

Figure 19 shows that E_{av} decreases proportionally with n. We get similar conclusions for D_{av} and T_L (Figures 20 and 21).

Comparing these last experiments, we can establish a compromise for optimising the Wave Gait, namely, that the robot should walk (in fact, it should "run", since $\beta < 50\%$) with $V_F \approx 1$ ms^{-1} and the mass of the robot should be concentrated on the body, while the legs should be as light as possible.

Finally, we compare the locomotion performance of several different animals (whose characteristics are presented in Appendix 1 [17 – 19]), based on the formulated indices.

The results (Figures 22 – 24) of the indices $\min[E_{av}(V_F)]$, $\min[D_{av}(V_F)]$ and $\min[T_L(V_F)]$ agree with the previous conclusions.

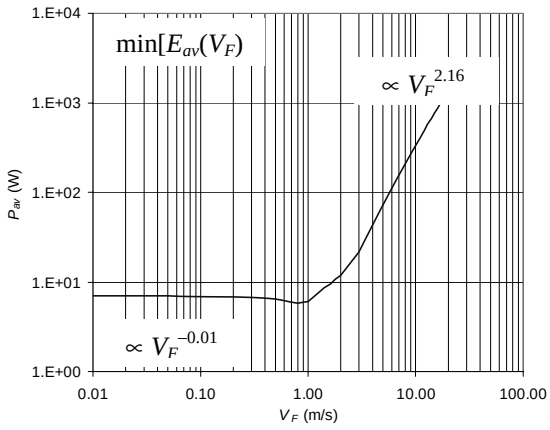

Figure 12: Plots of min[$E_{av}(V_F)$] for F_C = 0.01 m, *WG*

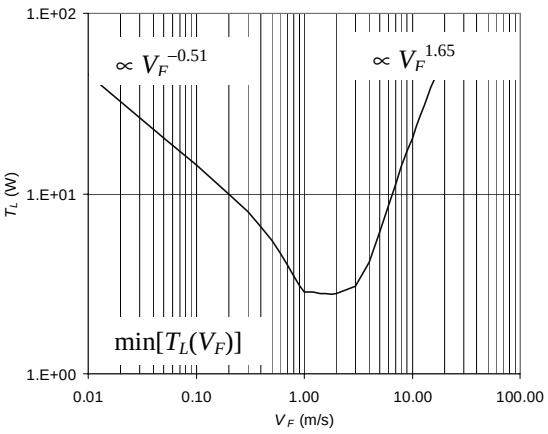

Figure 14: Plots of min[$T_L(V_F)$] for F_C = 0.01 m, *WG*

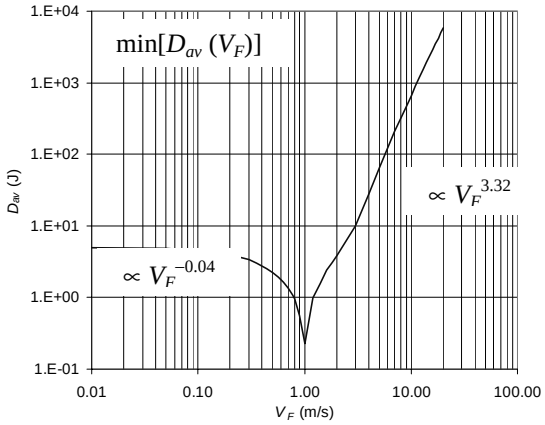

Figure 13: Plots of min[$D_{av}(V_F)$] for F_C = 0.01 m, *WG*

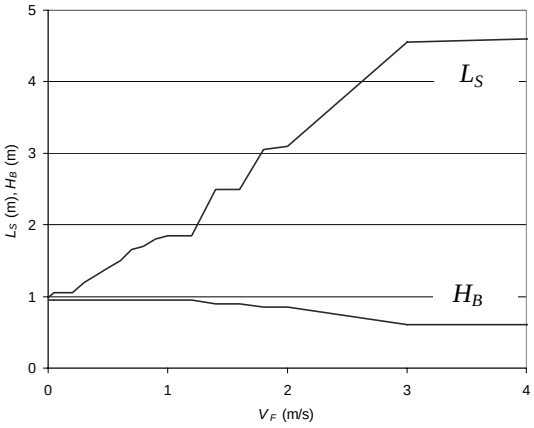

Figure 15: Plot of $L_S(V_F)$ and $H_B(V_F)$ for min(E_{av}) with F_C = 0.01 m, *WG*

5 Conclusions

In this paper we have compared various dynamic aspects of multi-legged robot locomotion gaits. By implementing different motion patterns, we estimated how the robot responds to a variety of locomotion variables such as duty factor, step length, body height, maximum foot clearance, foot trajectory offset and leg lengths. For analyzing the system performance three quantitative measures were defined: the average energy consumption, the mean power dispersion and the power expenditure in the actuators per walking distance. Analyzing the experiments we obtained the best set of locomotion variables and, also, we concluded that the results obtained through the different indices are compatible.

While our focus has been on a dynamic analysis in periodic gaits, certain aspects of locomotion are not necessarily captured by the proposed measures. Consequently, future work in this area will address the refinement of our models to incorporate more unstructured terrains, namely with distinct trajectory planning concepts. Moreover, we will also address the effects of the foot – ground interaction and a model describing the ground characteristics. The contact and reaction forces at the robot feet will enable further insight towards the development of efficient multi-legged locomotion robots.

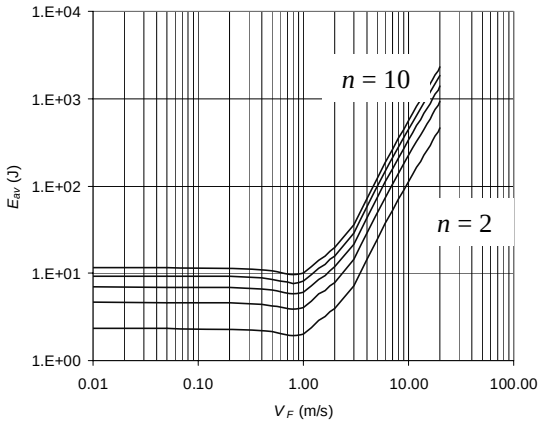

Figure 16: Plots of min[$E_{av}(V_F)$] *vs. n* for F_C = 0.01 m, *WG*

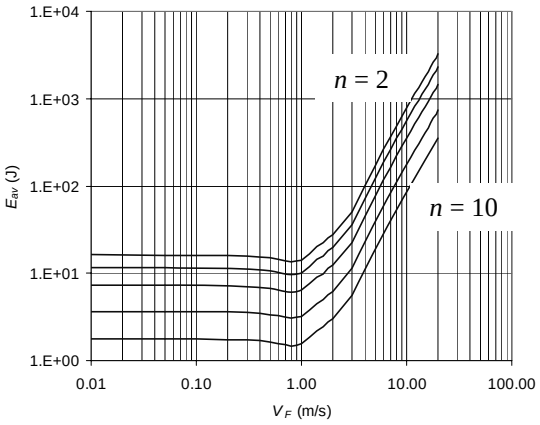

Figure 19: Plots of min[$E_{av}(V_F)$] *vs. n* for F_C = 0.01 m, *WG*

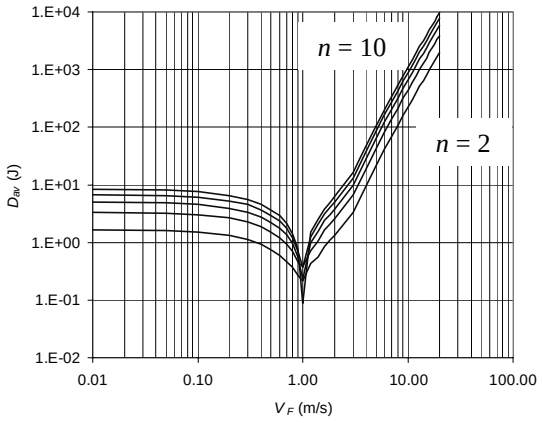

Figure 17: Plots of min[$D_{av}(V_F)$] *vs. n* for F_C = 0.01 m, *WG*

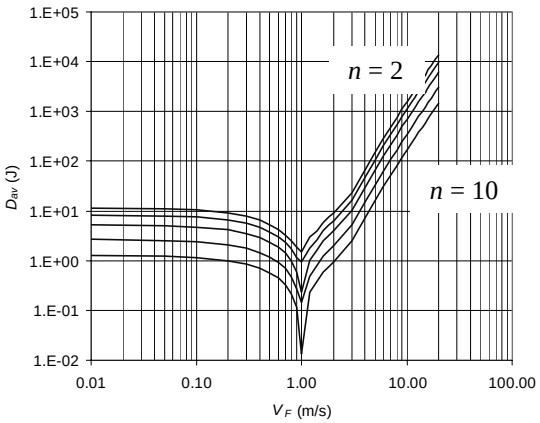

Figure 20: Plots of min[$D_{av}(V_F)$] *vs. n* for F_C = 0.01 m, *WG*

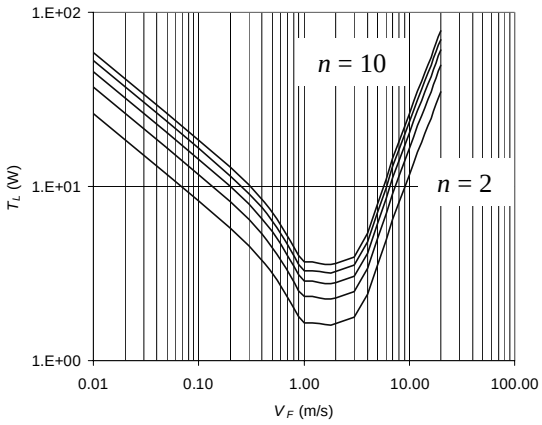

Figure 18: Plots of min[$T_L(V_F)$] *vs. n* for F_C = 0.01 m, *WG*

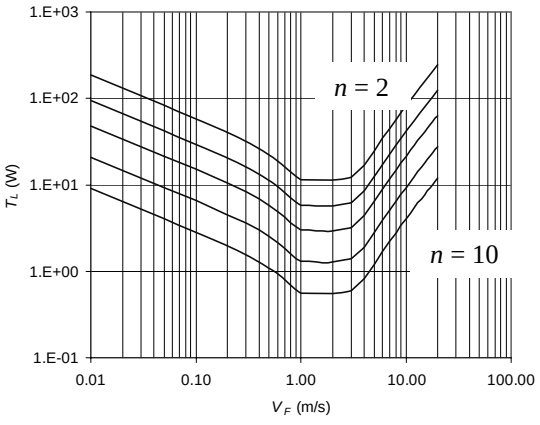

Figure 21: Plots of min[$T_L(V_F)$] *vs. n* for F_C = 0.01 m, *WG*

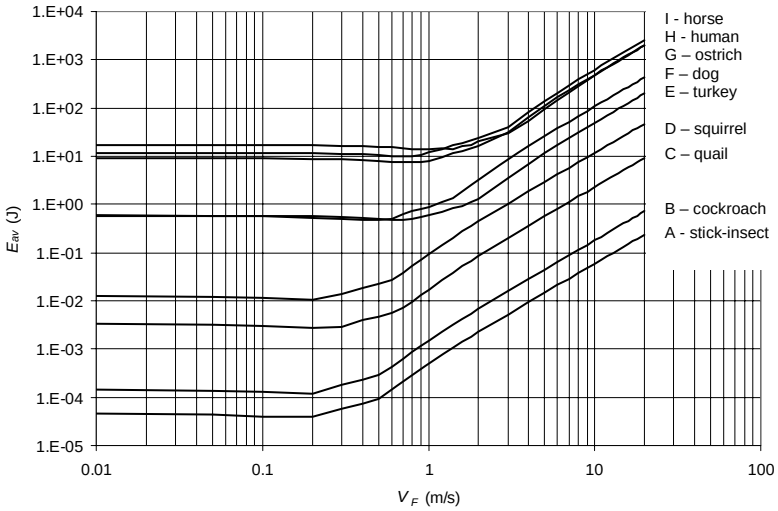

Figure 22: Plots of min[$E_{av}(V_F)$] *vs. n* for F_C = 0.01 m, *WG*

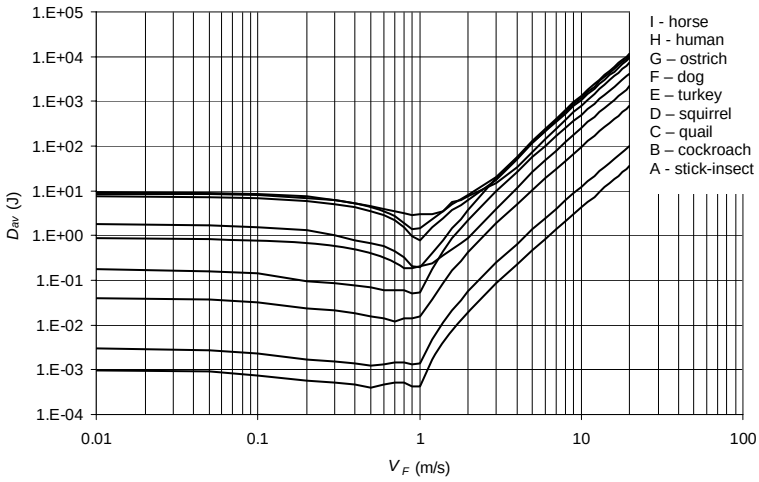

Figure 23: Plots of min[$D_{av}(V_F)$] *vs. n* for F_C = 0.01 m, *WG*

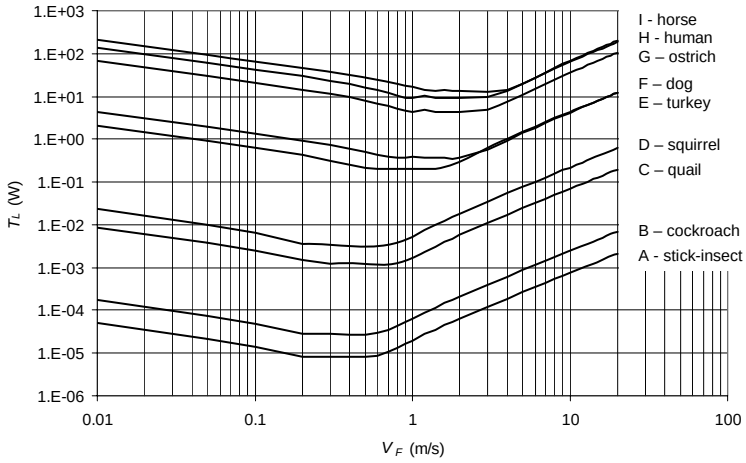

Figure 24: Plots of min[$T_L(V_F)$] *vs. n* for F_C = 0.01 m, *WG*

References

[1] D. J. Manko. *A General Model of Legged Locomotion on Natural Terrain*, Kluwer, Westinghouse Electric Corporation, 1992.

[2] S.-M. Song and K. J. Waldron. *Machines that Walk: The Adaptive Suspension Vehicle*, The MIT Press, 1989.

[3] D. Wettergreen and C. Thorpe. Gait Generation for Legged Robots. In *Proc. of the IEEE Int. Conf. on Intelligent Robots and Systems*, 1992.

[4] M. A. Jiménez and P. G. Santos. Terrain-Adaptive Gait for Walking Machines. *The Int. J. of Robotics Research*, 16 (3):320–339, 1997.

[5] Celaya, E. and Porta, J. M. A Control Structure for the Locomotion of a Legged Robot on Difficult Terrain. *IEEE Robotics & Automation Magazine*, 5 (2):43–51, 1998.

[6] Bai, S., Low, K. H. and Zielinska, T. Quadruped Free Gait Generation for Straight-Line and Circular Trajectories. *Advanced Robotics*. 13 (5):513–538, 1999.

[7] Inagaki, K. A Gait Study for a One-Leg-Disabled Hexapod Robot. *Advanced Robotics*. 12 (5):593–604, 1999.

[8] Tsukagoshi, H., Hirose, S. and Yoneda, K. Maneuvering Operations of a Quadruped Walking Robot on a Slope. *Advanced Robotics*. 11 (4):359–375, 1997.

[9] Yoneda, K., Suzuki, K., Kanayama, Y., Takahashi, H. and Akizono, J. Gait and Foot Trajectory Planning for Versatile Motions of a Six-Legged Robot. *Journal of Robotic Systems*. 14 (2):121–133, 1997.

[10] Marhefka, D. W. and Orin, D. E. Gait Planning for Energy Efficiency in Walking Machines. In *Proc. of the IEEE Int. Conf. on Robotics and Automation*, pages 474–480, USA, 1997.

[11] Chen, C.-H., Kumar, V. and Luo, Y.-C. Motion Planning of Walking Robots Using Ordinal Optimization. *IEEE Robotics & Automation Magazine*. 5 (2):22–32, 1998.

[12] Cho, D. J., Kim, J. H. and Gweon, D. G. Optimal Turning Gait of a Quadruped Walking Robot. *Robotica*. 13 (6):559–564, 1995.

[13] Bai, S., Low, K. H. and Teo, M. Y. Path Generation of Walking Machines in 3D Terrain. In *Proc. of the IEEE Int. Conf. on Robotics and Automation*, pages 2216–2221, USA, 2002.

[14] Silva, M. F., Machado, J. A. T. and Lopes, A. M. Energy Analysis of Multi-Legged Locomotion Systems. In *Proc. of the 4th Int. Conf. on Climbing and Walking Robots*, pages 143–150, Germany, 2001.

[15] Silva, M. F., Machado, J. A. T. and Lopes, A. M. Performance Analysis of Multi-Legged Systems. In *Proc. of the IEEE Int. Conf. on Robotics and Automation*, pages 2234–2239, USA, 2002.

[16] Silva, M. F., Machado, J. A. T. and Lopes, A. M. Power Analysis of Multi-Legged Systems. In *Proc. of the b'02 – 15th IFAC World Congress on Automatic Control*, Spain, 2002.

[17] M. A. Fedak, N. C. Heglund and C. R. Taylor. Energetics and Mechanics of Terrestrial Locomotion. II. Kinetic Energy Changes of the Limbs and Body as a Function of Speed and Body Size in Birds and Mammals. *Journal of Experimental Biology*. 79:23–40, 1982.

[18] R. Kram, B. Wong and R. J. Full. Three-Dimensional Kinematics and Limb Kinetic Energy of Running Cockroaches. *Journal of Experimental Biology*. 200:1919–1929, 1997.

[19] David A. Winter. *Biomechanics and Motor Control of Human Movement*, John Wiley & Sons, 1990.

Appendix 1

Number of Legs	Animal	Total Mass (Kg)	Leg and Body Mass (kg)	Leg lenghts (m)
	Quail	M_{Rt} = 0.0444	M_b = 0.036200	
			M_{i1} = 0.003600, i = 1, 2	L_{i1} = 0.026, i = 1, 2
			M_{i2} = 0.000500, i = 1, 2	L_{i2} = 0.026, i = 1, 2
	Turkey	M_{Rt} = 5.69	M_b = 4.220000	
			M_{i1} = 0.649000, i = 1, 2	L_{i1} = 0.21, i = 1, 2
			M_{i2} = 0.086000, i = 1, 2	L_{i2} = 0.21, i = 1, 2
n = 2 (Bipeds)				
	Ostrich	M_{Rt} = 89.5	M_b = 47.936000	
			M_{i1} = 18.271000, i = 1, 2	L_{i1} = 0.605, i = 1, 2
			M_{i2} = 2.515000, i = 1, 2	L_{i2} = 0.605, i = 1, 2
	Human	M_{Rt} = 80.0	M_b = 54.24	
			M_{i1} = 8.00, i = 1, 2	L_{i1} = 0.48, i = 1, 2
			M_{i2} = 4.88, i = 1, 2	L_{i2} = 0.48, i = 1, 2
	Squirrel	M_{Rt} = 0.11538	M_b = 0.089300	
			M_{i1} = 0.002700, i = 1, 2	L_{i1} = 0.024, i = 1, 2
			M_{i2} = 0.001540, i = 1, 2	L_{i2} = 0.024, i = 1, 2
			M_{i1} = 0.006400, i = 3, 4	L_{i1} = 0.024, i = 3, 4
			M_{i2} = 0.002400, i = 3, 4	L_{i2} = 0.024, i = 3, 4
	Dog	M_{Rt} = 5.0372	M_b = 3.705400	
			M_{i1} = 0.256700, i = 1, 2	L_{i1} = 0.1025, i = 1, 2
n = 4 (Quadrupeds)			M_{i2} = 0.081800, i = 1, 2	L_{i2} = 0.1025, i = 1, 2
			M_{i1} = 0.294900, i = 3, 4	L_{i1} = 0.1025, i = 3, 4
			M_{i2} = 0.032500, i = 3, 4	L_{i2} = 0.1025, i = 3, 4
	Horse	M_{Rt} = 97.904	M_b = 79.500000	
			M_{i1} = 3.571000, i = 1, 2	L_{i1} = 0.405, i = 1, 2
			M_{i2} = 1.887000, i = 1, 2	L_{i2} = 0.405, i = 1, 2
			M_{i1} = 2.720000, i = 3, 4	L_{i1} = 0.405, i = 3, 4
			M_{i2} = 1.024000, i = 3, 4	L_{i2} = 0.405, i = 3, 4
	Cockroach	M_{Rt} = 0.0026	M_b = 0.002250	
			M_{i1} = 0.000028, i = 1, 2	L_{i1} = 0.015305, i = 1, 2
			M_{i2} = 0.000005, i = 1, 2	L_{i2} = 0.015305, i = 1, 2
			M_{i1} = 0.000052, i = 3, 4	L_{i1} = 0.015305, i = 3, 4
			M_{i2} = 0.000009, i = 3, 4	L_{i2} = 0.015305, i = 3, 4
			M_{i1} = 0.000066, i = 5, 6	L_{i1} = 0.015305, i = 5, 6
			M_{i2} = 0.000014, i = 5, 6	L_{i2} = 0.015305, i = 5, 6
n = 6 (Hexapods)				
	Stick-insect	M_{Rt} = 0.0009	M_b = 0.000792	
			M_{i1} = 0.000019, i = 1, 2	L_{i1} = 0.0146, i = 1, 2
			M_{i2} = 0.000004, i = 1, 2	L_{i2} = 0.0146, i = 1, 2
			M_{i1} = 0.000014, i = 3, 4	L_{i1} = 0.0146, i = 3, 4
			M_{i2} = 0.000003, i = 3, 4	L_{i2} = 0.0146, i = 3, 4
			M_{i1} = 0.000014, i = 5, 6	L_{i1} = 0.0146, i = 5, 6
			M_{i2} = 0.000003, i = 5, 6	L_{i2} = 0.0146, i = 5, 6

About the Authors

Manuel F. Silva was born in April 11, 1970. He graduated and received the MSc. degree in electrical and computer engineering from the Faculty of Engineering of the University of Porto, Portugal, in 1993 and 1997, respectively. Presently he is Assistant Professor at the Institute of Engineering of the Polytechnic Institute of Porto, Department of Electrical Engineering. His research focuses on multi-legged walking robots.

J. A. Tenreiro Machado was born in October 6, 1957. He graduated and received the Ph.D. degree in electrical and computer engineering from the Faculty of Engineering of the University of Porto, Portugal, in 1980 and 1989, respectively. Presently he is Coordinator Professor at the Institute of Engineering of the Polytechnic Institute of Porto, Department of Electrical Engineering. His main research interests are robotics, modeling, control, genetic algorithms, fractional-order systems and intelligent transportation systems.

António M. Lopes received a Master's degree in electrical engineering and a doctoral degree in mechanical engineering both from the Porto University in Portugal in the years 1995 and 2000, respectively. His research interests include robot modeling and control, force-impedance control and non-linear control systems.